American Mineralogist, Volume 60, pages 375–390, 1975

An Experimental Study of Actinolite-Cummingtonite Phase Relations with Notes on the Synthesis of Fe-rich Anthophyllite

KENNETH L. CAMERON

Board of Earth Sciences, University of California, Santa Cruz, California 95064

Abstract

An amphibole quadrilateral, analogous to the well-known pyroxene quadrilateral, is defined by the end member compositions $Ca_2Mg_5Si_8O_{22}(OH)_2$ (tremolite), $Ca_2Fe_5Si_8O_{22}(OH)_2$ (ferrotremolite), $Mg_7Si_8O_{22}(OH)_2$ (anthophyllite), and $Fe_7Si_8O_{22}(OH)_2$ (grunerite). Phase relations along the join $Mg_{3.5}Fe_{3.5}Si_8O_{22}(OH)_2$–$Ca_2Mg_{2.5}Fe_{2.5}Si_8O_{22}(OH)_2$, through the center of the quadrilateral, were studied at P_{fluid} = 2 kbar and at oxygen fugacities defined by the FMQ buffer. Compositions along this join are expressed in mole percent of the calcic end member, actinolite (*e.g.*, Act_{70}). It has not been possible to bracket phase boundaries with reversals because of the reluctance of new phases to nucleate in crystalline starting materials.

Three amphiboles with intermediate Fe : Mg ratios—anthophyllite, cummingtonite, and actinolite—were synthesized. Cummingtonite and actinolite are separated by a solvus that is asymmetric with a very steep cummingtonite limb near Act_{10} and an actinolite limb that is measurably temperature dependent ($Act_{96\pm4}$ at 500°C, $Act_{85\pm4}$ at 600°C). The maximum solubility of the Ca-free component in the actinolite is reached at ~600°C. Actinolites with Fe : Mg ≅ 1, if coexisting with cummingtonites, are useful geothermometers and may be used to estimate, or put lower limits on, temperatures of metamorphism with a minimum uncertainty of ±35°C.

Actinolite decomposes by the reaction, actinolite → cummingtonite + clinopyroxene + quartz + H_2O. The products of this reaction differ from those reported for the decomposition of tremolite (Boyd, 1959) and ferrotremolite (Ernst, 1966).

Anthophyllite is the only amphibole which has been synthesized in Ca-free runs (*i.e.*, Act_0). The presence of Ca facilitates nucleation of cummingtonite, and the assemblage anthophyllite + cummingtonite grows at the expense of less stable assemblages between about Act_1 and Act_7. Cummingtonite alone is present at ~Act_{10}. Some experiments suggest that the absence of cummingtonite in Ca-free runs is only a nucleation problem, but the phase relations between the two Ca-poor amphiboles have not been resolved satisfactorily.

Introduction

Coexisting amphiboles have been reported from many metamorphic terranes, and much interest has developed concerning their compositions and phase relations (*e.g.*, Klein, 1968; Robinson and Jaffe, 1969; Ross, Papike, and Shaw, 1969; Robinson, Ross, and Jaffe, 1971; Stout, 1971). The compositions of many of these coexisting amphiboles lie in or near the system CaO–MgO–FeO–SiO_2–H_2O and can be depicted in an amphibole quadrilateral (Fig. 1) analogous to the familiar pyroxene quadrilateral. The three series of amphiboles that can be represented in this quadrilateral are (1) the Ca-rich monoclinic amphiboles tremolite-ferrotremolite, (2) the Ca-poor monoclinic amphiboles cummingtonite-grunerite, and (3) the Ca-poor orthorhombic amphiboles anthophyllite-ferroanthophyllite. The complete series tremolite-ferrotremolite is known from nature, and the two end members have been synthesized (Boyd, 1959; Ernst, 1966). Both series of Ca-poor amphiboles are stable at intermediate Fe: Mg, but neither pure-Fe ferroanthophyllite nor pure-Mg cummingtonite has been synthesized or found in nature. The approximate compositional limits of the two Ca-poor series are shown in Figure 1. In the following discussion Ca-rich and Ca-poor monoclinic amphiboles with intermediate Fe : Mg are referred to as actinolite and cummingtonite, respectively. Anthophyllite is used as a general term for all orthorhombic amphiboles.

Coexisting Ca-rich and Ca-poor amphiboles are

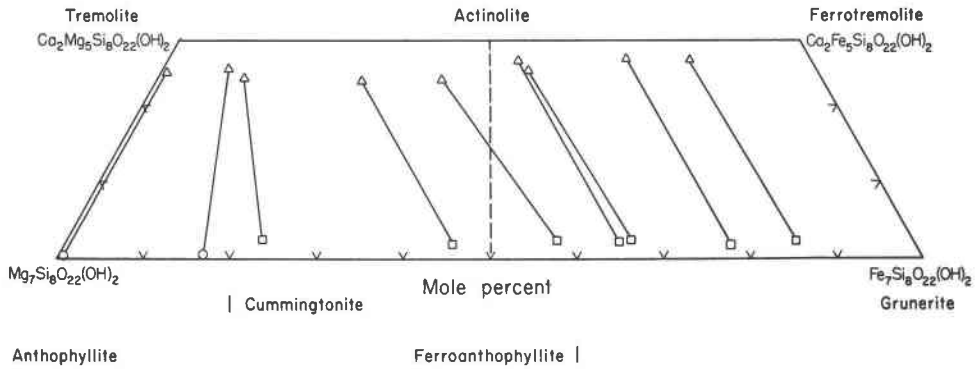

FIG. 1. The amphibole quadrilateral showing the compositions of some coexisting amphiboles that contain less than 2.5 wt percent Al_2O_3 and 1.8 wt percent MnO. Analyses of the most Fe-rich pair are given in Table 9; other analyses are from Klein (1968). Total Fe is assumed to be FeO. Dashed line indicates the join studied experimentally, $Mg_{3.5}Fe_{3.5}Si_8O_{22}(OH)_2$–$Ca_2Mg_{2.5}Fe_{2.5}Si_8O_{22}(OH)_2$. Symbols: circles, anthophyllite; squares, cummingtonite-grunerite; triangles, tremolite-actinolite. Compositional limits of the series cummingtonite-grunerite and anthophyllite-ferroanthophyllite are shown by vertical bars.

separated by a wide miscibility gap (Fig. 1) that is similar to the two-pyroxene field in the pyroxene quadrilateral. Some of these coexisting amphiboles contain exsolution lamellae indicating that their compositions depend on the temperature of equilibration; consequently, they may be useful as geothermometers.

Assemblages containing the two Ca-poor amphiboles, cummingtonite and anthophyllite, have also been reported (see Klein, 1968), and controversy has arisen concerning their phase relations. Some investigators (Eskola, 1950, p. 733; Boyd, 1959, p. 390) have proposed that the two amphiboles are polymorphs in the compositional range where both are stable. Others (Layton and Phillips, 1960, p. 660; Schürmann, 1968, p. 259) have concluded that a small amount of calcium is necessary to stabilize cummingtonite.

Amphiboles in the system CaO-MgO-FeO-SiO_2-H_2O were chosen for this experimental study because they are relatively simple chemically and are well represented in natural assemblages. The objectives of this study were twofold: (1) to determine the amount of solution between coexisting Ca-rich and Ca-poor monoclinic amphiboles as a function of temperature, and (2) to elucidate the phase relations between cummingtonite and anthophyllite. A join with intermediate Fe:Mg was required in order to satisfy the latter objective, and the join $Mg_{3.5}Fe_{3.5}Si_8O_{22}(OH)_2$-$Ca_2Mg_{2.5}$-$Fe_{2.5}Si_8O_{22}(OH)_2$ was chosen for study (Fig. 1). Compositions along this join are abbreviated henceforth as mole percentages of the calcic end member actinolite (*e.g.*, Act_{85}). The actual compositions of all amphiboles in multiphase assemblages will lie slightly off this join because Fe and Mg are not distributed equally between coexisting phases.

There have been several other experimental studies of phases or joins in this amphibole quadrilateral. Greenwood (1963), Boyd (1959), and Ernst (1966) determined the pressure-temperature stabilities of pure-Mg anthophyllite, tremolite, and ferrotremolite, respectively. Hinrichsen (1967), Schürmann (1967, 1968), and Hellner and Schürmann (1966) investigated the lower thermal stabilities, at P_{total} = 1000 bars, of the series anthophyllite-ferroanthophyllite, cummingtonite-grunerite, and tremolite-ferrotremolite, respectively. The bulk compositions of Hinrichsen's study were Ca-free, whereas those of Schürmann's (1967, 1968) contained 2.7 wt percent CaO. Popp, Gilbert, and Craig (1974) report cell parameters of synthetic amphiboles on the join $Mg_7Si_8O_{22}(OH)_2$–$Fe_7Si_8O_{22}(OH)_2$.

Experimental Techniques

Apparatus

Hydrothermal experiments were conducted with conventional "cold seal" equipment (Tuttle, 1949) at Virginia Polytechnic Institute and State University. Experiments employed both vertically and horizontally mounted furnaces. Temperatures were measured with bare-wire chromel-alumel thermocouples inserted in the end wall of the pressure vessels, read with a Leeds and Northrup Type K-4 potentiometer, and monitored with an Esterline Angus strip chart recorder. New thermocouple junctions were made before each run. Solid-state temperature controllers (Hadidiacos, 1969) were used with the horizontal furnaces and temperature fluctuations were generally no

more than ±1°C. West Instrument Corporation Model JPLT3 controllers were used with the vertically mounted Tem-Pres furnaces, and fluctuations were on the order of ±2° to 3°C. Several thermocouple-pressure vessel assemblies were calibrated at 1 atmosphere against the melting points of dried NaCl (800.4°C) and CsCl (646°C).

Pressure vessels were machined from the nickel-based alloy René 41, and a common pressure line connected them to a 5000 bar Heise pressure gauge. All runs were made at P_{total} = 2000 bars (±30 bars), and were brought to temperature and quenched isobarically. Runs were quenched by removing the pressure vessels from the furnaces and passing a stream of compressed air over them for about a minute. The temperatures of the pressure vessels were usually 200°C or less, 15–20 minutes after they were removed from the furnaces. There was no optical or other evidence to suggest that any reaction took place during the quench.

Oxygen fugacities were controlled by the fayalite-magnetite-quartz (FMQ) buffer utilizing the double capsule technique described in Eugster and Wones (1962). Inner capsules were $Ag_{70}Pd_{30}$; outer capsules were Au. At the completion of each run the buffers were checked optically for the assemblage fayalite-magnetite-quartz-H_2O.

Starting Materials

All charges were crystallized initially from either glass or an oxygen-balanced mix. These starting materials were prepared at compositional intervals of 10 mole percent actinolite along the join. Additional mixes were prepared on the compositions $Act_{1.25}$, $Act_{2.5}$, Act_5, Act_{15}, Act_{85}, and Act_{95}. The mixes were composed of Materials Research Corporation MgO; Johnson, Matthey and Co. grade I iron sponge; Fisher's "Certified" reagent $CaCO_3$ and Fe_2O_3; and Corning 7940 silica glass. The components of the mix were ground together for one hour under acetone with an agate mortar and pestle. Glasses were prepared at the Geophysical Laboratory under the supervision of the late Dr. J. F. Schairer.

Phase Identification and Characterization

Run products were examined optically using a polarizing microscope and white light. Refractive indices were determined in oils calibrated at intervals of 0.002 units below 1.70 and 0.005 above 1.70.

Charges were scanned routinely at 2°/min from 8° to 65° 2θ on a Norelco X-ray diffractometer equipped with a high intensity copper tube and a graphite monochromator. In addition, many charges were scanned at 1/8° per minute over critical 2θ ranges.

Unit cell parameters were determined using data from 3 oscillations (6 scans) run at 1/4 degree per minute with a time constant of 4, and with a spinel ($MgAl_2O_4$) internal standard (a = 8.083 Å) supplied by Professor G. V. Gibbs. The diffractometer tracings were at a scale of 1°2θ = 1 inch, and the positions of the peak tips were measured to 0.005°. The standard deviation of most peak positions was between 0.015° and 0.025°. Narrow, sharp peaks commonly had standard deviations of less than 0.010°, whereas the standard deviations of weak and/or irregular peaks were usually no larger than 0.035°. Unit cell parameters were refined using the computer program LSUCR (Evans, Appleman, and Handwerker, 1963). Copper $K\alpha$ wavelength (1.54180) was used below 40° 2θ and $K\alpha_1$ (1.54051) was used at higher angles. Reflections were weighted in the refinement by the factor $1/10000\sigma^2$ which gave a weight of 1.0 to peaks with standard deviations of 0.010. Unit cell parameters calculated using weighted reflections were usually within the error of the parameters calculated giving all reflections unit weights. Weighting was used in all cell refinements, however, because it gave slightly smaller standard errors and fewer reflections were rejected in the refinement.

Properties of Phases

Actinolite

Actinolite forms small crystals which are generally less than 5 microns long and 0.5 microns wide. Neither the precise refractive indices nor the extinction angle can be determined because of the small size of the crystals. However, the oil of refractive index 1.660 is intermediate between the α and γ indices of clumps of crystals in run 73B-100[1].

The presence of actinolite is established only by examination of X-ray diffractometer powder patterns. The powder pattern of a charge containing ~90 percent actinolite—the remainder being cummingtonite, clinopyroxene, and quartz—is shown in Figure 2A. The actinolite peaks were indexed by comparison with the calculated powder pattern of tremolite (Borg and Smith, 1969, p. 264). Actinolite is distinguished from the Ca-poor amphiboles by the position of the *310* peak at 28.4° (*cf* cummingtonite *310* and anthophyllite *610* both at about 29.1°). Reflections used to refine the cell parameters of actinolites are

[1] The number following the hyphen in the run number is the bulk composition of the charge expressed as mole percent actinolite.

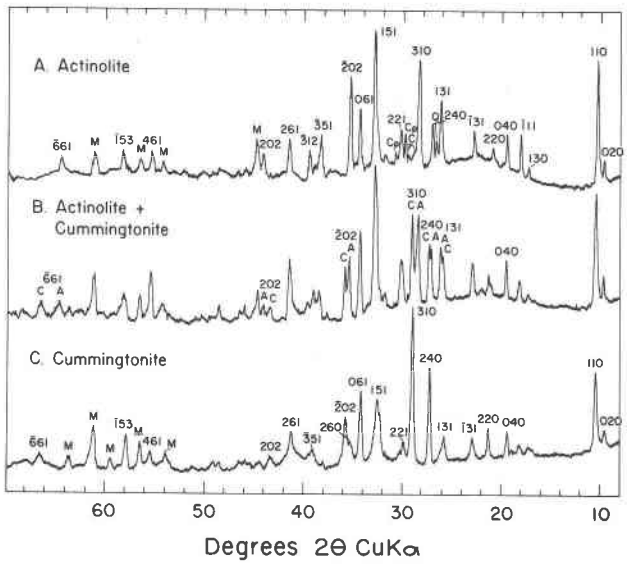

FIG. 2. X-ray diffractometer tracings of clinoamphiboles. (A) 80 percent actinolite + ?cummingtonite + clinopyroxene + quartz; run 73B-100, 558°C, 39 days. (B) actinolite + cummingtonite; run 46A-50, charge run at 3 different temperatures: 655°C–46 days, 700°C–14 days, 500°C–13 days; total time, 73 days. (C) cummingtonite, run 55D-10, 620°C, 102 days. Abbreviations: A-actinolite, C-cummingtonite, Cp-clinopyroxene, Q-quartz, M-multiple reflection. Instrument settings: Cu$K\alpha$ radiation; 40 kV; 20 mA; 200 cps; time constant, 16; scan speed, 1/8 degree 2θ per minute; chart speed, 1/16 an inch per minute.

given in Table 1. Where clinopyroxene plus other products exceeded 25 percent, the actinolite $\bar{2}02$ and *202* reflections were not used because of the interference of strong clinopyroxene peaks. Cell parameters of an actinolite believed to be on or very near the composition $Ca_2Mg_{2.5}Fe_{2.5}Si_8O_{22}(OH)_2$ are given in Table 2. Also included are the cell

TABLE 1. Reflections Used to Refine Unit Cell Parameters of Actinolite and Cummingtonite

	Actinolite Run 73B-100		Cummingtonite Run 55D-10		
$h\ k\ l$	$2\theta_{obs}$	$2\theta_{cal}$	$2\theta_{obs}$	$2\theta_{cal}$	$2\theta^{act}_{obs}-2\theta^{cum}_{obs}$
$0\ \bar{4}\ 0$	19.54	19.52	19.56	19.54	0.02
$\bar{1}\ 3\ 1$	22.84	22.83	23.01	23.02	0.17
$1\ 3\ 1$	26.21	26.21	25.93	25.92	0.28
$2\ 4\ 0$	27.04	27.05	27.40	27.41	0.36
$3\ 1\ 0$	28.38	28.40	29.14	29.15	0.76
$0\ 6\ 1$	34.37	34.37	34.26	34.28	0.11
$\bar{2}\ 0\ 2$	35.30	35.31	35.82	35.81	0.50
$2\ 6\ 1$	41.49	41.46	41.31	41.31	0.18
$2\ 0\ 2$	44.11	44.08	43.35	43.32	0.76
$\bar{6}\ 6\ 1$	64.39	64.36	66.59	66.54	2.20

Cu$K\alpha$ radiation below 40°2θ; Cu$K\alpha_1$ above 40°

parameters for such an amphibole derived from those of the synthetic end-members tremolite-ferrotremolite[2] (Ernst, 1968, p. 13) assuming a linear relationship between the cell parameters and Fe content.

Cummingtonite

Cummingtonite crystals are generally somewhat larger than those of actinolite, and they reach a maximum size of ~15 × 3 microns. Nevertheless, when both amphiboles are present, they cannot be distinguished optically with confidence. The extinction angle, $Z \wedge c$, of cummingtonite (163A-10) is 15°, and the refractive indices are $\alpha = 1.650(3)$ and $\gamma = 1.668(3)$[3].

The X-ray powder pattern of cummingtonite

[2] The values given in Ernst (1968, p. 13) for the *a* axis, d_{100} and *V* of ferrotremolite should be 9.97Å, 9.65Å, and 939Å respectively (Ernst, 1966, p. 43).

[3] The uncertainty in the refractive index is given in parentheses and refers to the last digit.

TABLE 2. Unit Cell Parameters

	a(Å)	b(Å)	c(Å)	β (°)	V(Å^3)	d_{100}(Å)
Actinolite[a]	9.892(5)*	18.191(12)	5.295(3)	104.65(5)	921.9(7)	9.572(5)
Actinolite[b]	9.903	18.200	5.286	104.51	922.0	9.582
Cummingtonite[c]	9.544(5)	18.171(8)	5.316(3)	102.33(5)	900.8(6)	9.324(5)
Cummingtonite[d]	9.526(9)	18.190(13)	5.320(5)	102.04(6)	901.5(1)	9.316(0)
Anthophyllite[e]	18.622(12)	18.185(21)	5.309(5)	90.0	1797.7(21)	9.311**
Pure-Mg Anthophyllite[f]	18.608(35)	17.964(59)	5.303(12)	90.0	1772.5(62)	9.304**
Pure-Mg Anthophyllite[g]	18.61(2)	18.01(6)	5.24(1)	90.0	1756.2	9.305**

a) Actinolite, 73B-100, 558°C, 39 days
b) Actinolite, predicted - see text
c) Cummingtonite, 55D-10, 620°C, 102 days
d) Cummingtonite, predicted (Klein & Waldbaum, 1967)
e) Anthophyllite, 30C-0, 675°C, 44 days
f) Pure-Mg anthophyllite, new parameters, see Table 4.
g) Pure-Mg anthophyllite (Greenwood, 1963)

*Calculated standard errors are given in parentheses and refer to the last decimal place(s).
**d_{200}

(Figures 2C and 3A) was indexed by comparison with the calculated powder pattern of cummingtonite in Borg and Smith (1969, p. 372). Cummingtonite is distinguished from actinolite by its *310* peak at 29.1°2θ (Fig. 2B), and from anthophyllite by its *131* peak at 26.0° 2θ (*cf* Figs. 3A, 3C). Cell parameters of cummingtonite, $Ca_{0.2}Mg_{3.4}Fe_{3.4}Si_8O_{22}(OH)_2$, are given in Table 2 along with those calculated using the equations of Klein and Waldbaum (1967). The reflections used to determine the cell parameters are listed in Table 1.

Estimation of the Compositions of Clinoamphiboles in Multiphase Assemblages

Figure 2B shows the powder pattern of a charge that contains nearly 100 percent amphibole and is composed of subequal amounts of actinolite and cummingtonite. Six relatively strong clinoamphibole peaks—*131, 240, 310, $\bar{2}02$, 202,* and *$\bar{6}61$*—show measurable separation (see Table 1 for approximate separations). Where cummingtonite and actinolite are present in subequal amounts, a unique 2θ can be measured for each of the above peaks; thus it is possible to determine unit cell parameters of both amphiboles. No correction is made for overlap of peaks. The *040* peak, which shows no separation (Fig. 2B), is also measured and included in the refinement of both amphiboles. The inclusion of the *040* peak has little effect on the value of *b*, but it does significantly reduce the standard error of *b*.

The important chemical variables of the coexisting actinolite and cummingtonite are Ca content and Fe : Mg ratio. Both X-ray powder and electron microprobe methods have been used to estimate the compositions of the amphiboles in this study. Colville, Ernst, and Gilbert (1966, p. 1741) have shown that, within any given amphibole series, the *b* axis increases with replacement of Fe for Mg in the *M*(2) site. The *b* axis was chosen to estimate the Fe content of amphiboles in this study because relative to other cell parameters it shows a large change in length with varying Fe : Mg. Moreover, the first four entries in Table 2 show that, at the Fe : Mg of this study, variation in Ca has little effect on the *b* axes of the clinoamphiboles. Klein and Waldbaum (1967) have shown that in the series cummingtonite–grunerite there is a linear relation between Fe content and the *b* cell dimension. Their determinative curve, which has a standard error of about ±2.5 mole percent of the Fe end-member, is used to estimate the Fe content of cummingtonites in this study.

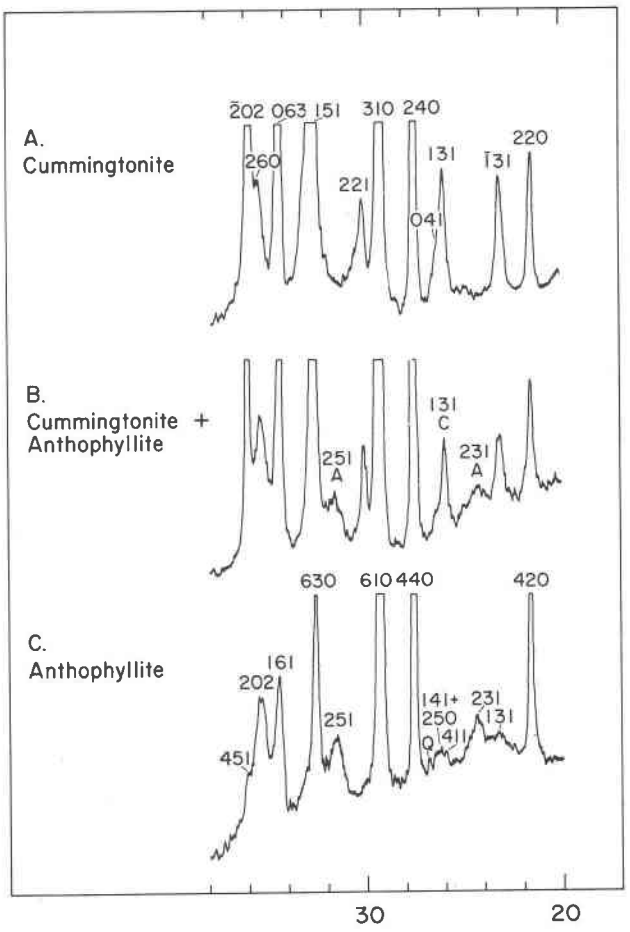

FIG. 3. X-ray diffractometer tracings of Ca-poor amphiboles. (A) cummingtonite, run 55D-10, 620°C, 102 days. (B) cummingtonite + anthophyllite, run 118C-1.25, 667°C, 60 days. (C) anthophyllite, run 30C-0, 675°C, 44 days. Instrument settings: Cu*K*α radiation; 40 kV; 30 mA; 100 cps; time constant, 16; scan speed, 1/8 degree 2θ per min.; chart speed, 1/16 an inch per min. Abbreviations: A-anthophyllite; C-cummingtonite; Q-quartz.

A comparison of the *b* cell dimensions of tremolite (18.054Å, Ernst, 1968, p. 13), actinolite with Fe : Mg = 1 (18.191Å, Table 2), and the average value of *b* for ferrotremolite (18.34Å, Ernst, 1966) suggests that in the series tremolite–ferrotremolite there is also a linear relationship between Fe content and *b*, and such a determinative curve was used in this study. Ernst reports a range in *b* from 18.31 to 18.39 Å for ferrotremolite; these values result in an uncertainty of ±5 mole percent of the Fe end-member at Fe : Mg = 1.

Calcium is confined to the *M*(4) site in amphiboles, and Whittaker (1960) and Gibbs (in Appleman *et al*, 1966) have shown that among the different

amphibole series the β angle is related to the mean ionic radius of the cations in $M(4)$. In this study linear relations were tested between the cell parameters and Ca contents of three charges that had been converted largely to a single amphibole (cummingtonite, 55D-10, 99 percent; actinolite, 53D-80, 85 percent; and actinolite, 73B-100, 90 percent). The calculated d_{100} ($a \sin \beta$) proved to be the best estimator of the Ca content of the charge and presumably of the amphibole; therefore, d_{100} rather than the β angle was used to estimate the Ca-content of the amphiboles.

A linear determinative curve for Ca *vs* d_{100} was constructed using the data from 55D-10 and 73B-100. The calcium content of the amphiboles is expressed as mole percent actinolite $Ca_2(Mg,Fe)_5Si_8O_{22}(OH)_2$ with an unspecified Fe : Mg. The d_{100} standard error of most amphiboles in this study is ≤ 0.01 which introduces an uncertainty of ± 4 mole percent actinolite assuming that there is no error in the determinative curve.

The amphiboles synthesized in this study are too small for conventional electron microprobe analysis. Nevertheless it is possible to make partial analyses of such material using an intensity ratio method recently discussed in detail by Eugster *et al* (1972). Analyses in this study were made at the State University of New York at Stony Brook using an ARL-EMX-SM electron microprobe. Intensity data were collected simultaneously for Ca, Fe, Mg, and Si. Calibration curves, calculated using the correction procedure of Bence and Albee (1968), were used to relate the observed intensity ratios—Ca/Si, Fe/Si, and Mg/Si—to the Ca contents and Fe-Mg ratios of the synthetic amphiboles.

Anthophyllite

Anthophyllite crystals average 5–10 microns long and 1–2 microns wide, but crystals up to 20 microns in length have been observed. Refractive indices of anthophyllite—$\alpha = 1.650(3)$, $\gamma = 1.666(3)$—are identical, within error, to those of cummingtonite. Anthophyllite crystals, being orthorhombic, have parallel extinction in many orientations, but they can have inclined extinction when planes of the type (*hkl*) are parallel to the microscope stage (Johannsen, 1937, p. 212).

The powder pattern of anthophyllite (Fig. 3C) was indexed by comparison with that calculated for anthophyllite by Borg and Smith (1969, p. 406). It differs from that of cummingtonite by the presence of the rather weak *231* (24.2° 2θ) and *251* (31.5° 2θ) peaks, and by the conspicuous absence of the relatively strong monoclinic amphibole *131* peak near 26.0° 2θ (*cf* Fig. 3A, 3C). There is a small irregular peak near 26°2θ in all powder patterns of anthophyllite, but this is believed to be the combined effect of the *411, 141,* and *250* orthoamphibole peaks that have calculated 2θ values of 25.9°, 26.2°, and 26.3°, respectively, for the anthophyllite of this study. The *141* and *250* peaks have a calculated combined intensity of 6 (Borg and Smith, 1969, p. 406) which is greater than that observed. In cummingtonite-anthophyllite assemblages, the cummingtonite *131* peaks can be seen superimposed on the low anthophyllite peak (Fig. 3B).

The calculated intensities of cummingtonite and actinolite peaks are in good agreement with those observed; however, the calculated intensities of many anthophyllite peaks are considerably greater than observed. For example, the calculated intensities of the *020, 231,* and *251* reflections are 84, 53, and 58 respectively, whereas the observed intensities are ≤ 15, which is in good agreement with those reported by Greenwood (1963) for pure-Mg anthophyllite.

Cell dimensions of anthophyllite, $Mg_{3.5}Fe_{3.5}Si_8O_{22}(OH)_2$, synthesized in this study are presented in Table 2, and the reflections used in the refinement are given in Table 3. Indexing of anthophyllite peaks in powder patterns is particularly difficult because of the myriad reflections permitted by the primitive cell, and the calculated pattern (Borg and Smith, 1969) suggests that some of Greenwood's anthophyllite peaks are incorrectly indexed. These were reindexed (Table 3) and new cell parameters were calculated. Except for c, the parameters are identical, within error, to those reported by Greenwood (Table 2).

Other Phases

Orthopyroxene forms bladed crystals averaging 30μ long and is readily detected in X-ray scans by the presence of the *420* peak at 27.9°2θ.

Clinopyroxene, present as small equant crystals about 5–10μ in size, is identified in X-ray scans by its $\bar{2}21$ peak at 29.7° 2θ. The precise composition of the clinopyroxene is not known, but it always coexists with a less calcic phase such as actinolite, cummingtonite, and/or orthopyroxene. Natural metamorphic clinopyroxenes that coexist with these phases contain 10–15 percent hypersthene in solid solution.

Talc, cristobalite, magnetite, olivine, and a carbonate mineral were crystallized from mixes at low temperatures. Cristobalite was found only in runs of

TABLE 3. Reflections Used to Refine Unit Cell Parameters of Anthophyllite

Anthophyllite (this study)				Anthophyllite, Greenwood (1963)				
h k l	d(calc) Å	d(obs) Å	I/Io	h k l	d(calc) Å	d(obs) Å	d(calc)*	I/Io
0 2 0	9.0922	9.0705	5	2 0 0	9.304	9.213	8.982R	5
2 1 0	8.2879	8.3224	35	2 1 0	8.266	8.330	8.262	70
0 4 0	4.5461	4.5388	10	4 1 0	4.504	4.494	4.491	35
4 2 0	4.1439	4.1481	15	4 2 0	4.133	4.141	4.131	5
2 3 1	3.6704	3.6765	5	4 3 0	3.677	3.657	3.651	15
4 4 0	3.2526	3.2514	50	4 4 0	3.235	3.228	3.231	50
6 1 0	3.0595	3.0612	100	6 1 0	3.056	3.064	3.056	100
				5 2 1	2.875	2.872	2.885	15
6 3 0	2.7626	2.7616	20	4 4 1	2.753	2.750	2.754	10
1 6 1	2.6062	2.6121	20					
2 0 2	2.5528	2.5480	15	2 0 2	2.522	2.536	2.550	5
9 6 1	1.6267	1.6254	10					
0 5 3	1.5913	1.5918	15					

*Calculated using indices shown for anthophyllite, this study
R Rejected in refinement
CuKα radiation below 40°2θ; CuKα$_1$ above 40°

less than two weeks duration, whereas longer runs produced quartz.

Phase Relations

Introduction

Phase relations along the join $Mg_{3.5}Fe_{3.5}Si_8O_{22}(OH)_2$-$Ca_2Mg_{2.5}Fe_{2.5}Si_8O_{22}(OH)_2$ are shown in Figure 4. Explanation of abbreviations used in the following figures, tables, and text are given in Table 4.

It has not been possible to bracket any field boundaries in Figure 4 with reversal runs because of the reluctance of new phases to nucleate in crystalline starting material. However, in many runs (triangles, Fig. 4) the starting assemblage was changed during the run by the loss of one or more phases, and in some cases these set either minimum or maximum limits for boundary curves.

The open symbols in Figure 4 represent synthesis data, because the final assemblage was not produced from an assemblage stable in an adjacent field. Most of these open symbols, however, indicate *run series*, that is, charges that have been rerun several times at the same temperature. It was necessary to rerun charges because mix and glass starting materials usually produce mixtures of amphiboles plus carbonate-free anhydrous phases when run between ~550-750°C. When the charges were rerun, the amphiboles usually grew at the expense of the anhydrous phases; therefore, most charges were rerun until the assemblage was changed by the loss of one or more anhydrous phases and/or until the proportion of phases stopped changing.

The letter in the run number (Table 5) indicates the number of times that the charge was rerun as close as possible to the same temperature; thus, A indicates that the charge was run only once, whereas D indicates that the charge was run four times. The assemblage listed under "Solid starting material" (Table 5) for run series (*i.e.*, runs with a B or higher letter in the run number) is the *product* of the *first* run of the series. This is the starting assemblage for the following runs of the series. The temperatures shown in Table 5 are for the final run of the series. Unless otherwise indicated the uncertainty due to temperature fluctuations during runs, and temperature variation from run to run, are less than ±3°C.

The total percentages of amphibole(s) in both the starting and final assemblages (Table 5) are "eyeball" estimates made principally from X-ray scans; however, they were found to be reproducible to about ±10 percent at mid range, and to ±5 percent at the lower (10 percent) and upper (90 percent) extremes. Five percent of a phase generally indicates that it is barely, but definitely, detectable on the X-ray scan; one percent indicates that it is detectable only optically and then as scattered grains. No claim is made that these estimations are correct in an absolute sense, but they are useful in demonstrating the amount of reaction that took place.

Actinolite-Cummingtonite Phase Relations

The phase relations involving actinolite, cummingtonite, and their dehydration assemblages are shown in Figure 4. Reaction rates were more sluggish, and amphibole yields were generally lower, in Ca-rich charges than Ca-poor ones. Several charges less

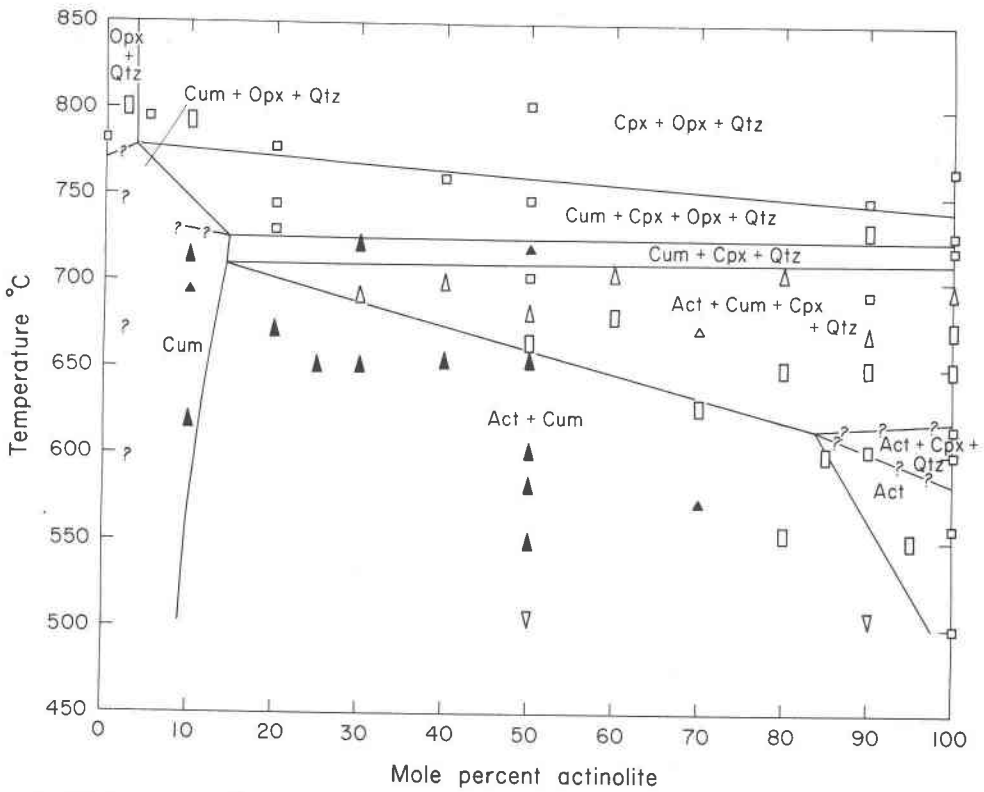

FIG. 4. Phase diagram for the pseudobinary join, $Mg_{3.5}Fe_{3.5}Si_8O_{22}(OH)_2$-$Ca_2Mg_{2.5}Fe_{2.5}Si_8O_{22}(OH)_2$+ excess H_2O, at P_{fluid} = 2000 bars and at oxygen fugacities defined by the FMQ buffer. All assemblages coexist with a vapor phase. Symbols: solid triangles, final assemblage produced from a starting assemblage stable in an adjacent field—the apex of the triangle pointing to the boundary separating the fields; open triangles that point up, Act+Cum+Cpx+Qtz produced by loss of Opx from the assemblage Act+Cum+Cpx+Opx+Qtz; open triangles that point down, Act+Cum produced from an assemblage containing talc; open rectangles, all other synthesis runs. Approximate temperature uncertainty shown by height of symbol. Abbreviations are given in Table 4.

calcic than Act_{60} were converted to about 99 percent amphibole(s) in runs of 40 to 60 day durations (Table 5).

Cummingtonite appears to be the only amphibole present in charges with the bulk composition of Act_{10} (Figs. 2C, 3A). These charges contain 1.27 wt percent CaO. A field of Act + Cum exists between about Act_{10} and Act_{90}, with the actinolite limb of the solvus being more temperature-sensitive than the cummingtonite limb. The determination of the solvus is discussed in a later section. Because the join studied is not parallel to the slope of the tielines that connect coexisting actinolite and cummingtonite (Fig. 1), the amphiboles at any given temperature become more magnesium rich as the bulk compositions become less calcic. Consequently, it is possible for actinolites on the Ca-poor side of the diagram to have a higher thermal stability than those on the Ca-rich side; and as a result the upper boundary for the field Act+Cum rises to the Ca-poor side.

Most charges run in the field Act (Fig. 4) have produced relatively low yields of amphibole (Table 5). The maximum yield of actinolitic amphibole, estimated as ~90 percent (Fig. 2A; run 73B-100) was produced at 558°C using as starting material Tc+Cc+Crist+Mag, seeded with about 10 percent

TABLE 4. Abbreviations Used in Tables, Text, and Following Figures

Act	= actinolite	Grun	= grunerite
Anth	= anthophyllite	Hem	= hematite
Carb	= carbonate (undifferentiated)	Hd	= hedenbergite
Cc	= calcite	Mag	= magnetite
Cpx	= clinopyroxene	Ol	= olivine
Crist	= cristobalite	Opx	= orthopyroxene
Cum	= cummingtonite	Qtz	= quartz
Fa	= fayalite	Tc	= talc
Ferrotre	= ferrotremolite	Tre	= tremolite

Act+Cpx+Qtz from a previous run. When the charge was rerun, however, the actinolite showed no signs of growth at the expense of the remaining 10 percent Cum+Cpx+Qtz. Similarly seeded runs using "oxide" mix and glass as starting material produced 70 and 30 percent actinolite respectively at ~550°C.

It has not been possible to locate with accuracy the upper boundary of the field Act because of the metastable persistence of cummingtonite, clinopyroxene, and quartz at temperatures (500°-550°C) where actinolite alone is presumably stable and because actinolite, once crystallized, will not react to form its breakdown products except at relatively high temperatures (700°C). A field of Act+Cpx+Qtz is believed to separate the fields of Act and Act+Cum+Cpx+Qtz, but runs within the boundaries of this field (Fig. 4) have all produced the three appropriate phases plus cummingtonite.

Using Figure 5 it can be easily shown that the field Act+Cpx+Qtz should separate the fields of Act and Act+Cum+Cpx+Qtz. In this schematic isothermal-isobaric section the assemblage Act+Cum+Cpx

TABLE 5. Run Data for the Join, $Mg_{5.5}Fe_{3.5}Si_8O_{22}(OH)_2$–$Ca_2Mg_{2.5}Fe_{2.5}Si_8O_{22}(OH)_2$ + excess H_2O, at P_{fluid} = 2000 Bars and at Oxygen Fugacities Defined by the Fayalite-Magnetite-Quartz Buffer[1]

Run no.*	Solid starting material	Temp. (°C)	Total Duration (days)	Percentage amphiboles start	final	Final crystalline assemblage**
		Field: Cum				
55D-10	Cum+Opx+Qtz	620‡	102	50	99	Cum+(Opx+Qtz)
163A-10	Cum+Opx+Qtz	694	19	80	98	Cum+(Qtz)
148C-10	Cum+Opx+Qtz	715‡	50	70	98	Cum+(Qtz)
		Field: Act+Cum				
128B-20	Act+Cum+Cpx+Qtz	672‡	50	95	99	Act+Cum+(Cpx+Qtz)
87C-25	Act+Cum+Cpx+Qtz	652‡	40	95	99	Act+Cum+(Cpx+Qtz)
42C-30	Act+Cum+Cpx+Qtz	653‡	73	90	97	Act+Cum+(Cpx+Qtz)
35C-40	Act+Cum+Cpx+Qtz	655‡	65	85	95	Act+Cum+(Cpx+Qtz)
16E-50	Act+Cum+Tc+Cc+Qtz+Mag+Ol	505‡	111	10	99	Act+Cum+(Tc+Qtz+Mag)
17D-50	Act+Cum+Cpx+15% excess Qtz	550‡	81	70	84	Act+Cum+(Cpx+15% excess Qtz)
18C-50	Act+Cum+Cpx+Qtz	582‡	47	90	99	Act+Cum+(Cpx+Qtz)
15B-50	Act+Cum+Cpx+Qtz	603‡	47	90	99	Act+Cum+(Cpx+Qtz)
13B-50	Act+Cum+Cpx+Qtz	655‡	46	90	98	Act+Cum+(Cpx+Qtz)
164A-70	Act+Cum+Cpx+Qtz	571	15	90	95	Act+Cum+(Cpx+Qtz)
129C-70	Act+Cum+Cpx+Qtz	627‡	60	70	85	Act+Cum+(Cpx+Qtz)
38C-80	Act+Cum+Cpx+Qtz	556‡	47	95	97	Act+Cum+(Cpx+Qtz)
132C-85	Act+Cum+Cpx+Qtz	600‡	61	50	75	Act+Cum+(Cpx+Qtz)
92D-90	Act+Tc+Cc+Qtz	505‡	80	10	95	Act+Cum+(Cpx+Qtz)
		Field: Act				
117C-95	Act+?Cum+Cpx+Qtz	550‡	60	60	85	Act+(Cum+Cpx+Qtz)
51B-100	Act+Cpx+Qtz	500	58	50	75	Act+(Cpx+Qtz)
11A-100	mix + seed	552‡	12		70	Act+Cpx+Qtz
73B-100	Tc+Crist+Cc+Mag+10% seed 11A-100	558	39	90	90	Act+(?Cum+Cpx+Qtz)
190B-100	Act+Cpx+Qtz+?Cum	552	164	75	90	Act+(Cpx+Qtz)
		Field: Act+Cpx+Qtz				
71B-90	Act+Cum+Cpx+Qtz	600‡	39	10	25	Act+Cpx+Qtz+5% (Cum)
130A-100	mix + seed 73B-100	600	26		25	Act+Cpx+Qtz+5% (Cum+?Opx)
93B-100	Act+Cum+Cpx+Qtz	614	28		30	Act+Cpx+Qtz+15% (Cum)
		Field: Act+Cum+Cpx+Qtz				
96C-30	?Act+Cum+Cpx+Opx+Qtz	692‡	42	60	90	?Act+Cum+Cpx+Qtz
40C-40	?Act+Cum+Cpx+Opx+Qtz	699‡	62	75	85	?Act+Cum+Cpx+Qtz
43D-50	Act+Cum+Cpx+Qtz	665‡	101	75	95	Act+Cum+Cpx+Qtz
81C-50	?Act+Cum+Cpx+Opx+Qtz	684‡	43	75	85	Act+Cum+Cpx+Qtz
19B-50	Act+Cum+Cpx+Qtz	702	44	75	85	Act+Cum+Cpx+Qtz
56C-60	Act+Cum+Cpx+Qtz	681‡	81	70	85	Act+Cum+Cpx+Qtz
37C-60	Act+Cum+Cpx+Opx+Qtz	704	54	40	70	Act+Cum+Cpx+Qtz
84B-70	Act+Cum+Cpx+Qtz	627‡	29	50	60	Act+Cum+Cpx+Qtz
53D-80	Act+?Cum+Cpx+Qtz	651‡	81	70	85	Act+Cum+Cpx+Qtz
89C-80	Act+Cum+Cpx+Opx+Qtz	705‡	47	20	40	Act+Cum+Cpx+Qtz

[1] *See Table 4 for abbreviations.*

TABLE 5. Continued

Run no.*	Solid starting material	Temp. (°C)	Total Duration (days)	Percentage amphiboles start	final	Final crystalline assemblage**
	Field: Act+Cum+Cpx+Qtz (Continued)					
52E-90	Act+Cum+Cpx+Qtz	650‡	109	60	80	Act+Cum+Cpx+Qtz
82C-90	Act+Cum+Cpx+Opx+Qtz	671‡	44	15	25	Act+Cum+Cpx+Qtz
64B-90	Act+Cum+Cpx+Qtz	692	39	20	30	Act+Cum+Cpx+Qtz
60C-100	Act+?Cum+Cpx+Qtz	649‡	50	50	75	Act+?Cum+Cpx+Qtz
34D-100	Act+Cum+Cpx+Qtz	652	71	15	25	Act+Cum+Cpx+Qtz
105C-100	Act+Cum+Cpx+Qtz	671‡	46	20	25	Act+Cum+Cpx+Qtz
103B-100	Act+Cum+Cpx+Opx+Qtz	695‡	26	10	15	Act+Cum+Cpx+Qtz
	Field: Cum+Cpx+Qtz					
85C-30	Cum+Cpx+Opx+Qtz	722‡	43	75	90	Cum+Cpx+Qtz+1% (Opx)
77B-50	?Act+Cum+Cpx+Opx+Qtz	720	32	50	70	Cum+Cpx+Qtz+5% (Opx+?Act)
100B-70	?Act+Cum+Cpx+Opx+Qtz	721	31	15	20	Cum+Cpx+Qtz+10% (Opx+?Act)
140B-100	Act+Cpx+Qtz	718	38	70	30	Cum+Cpx+Qtz+20% (Act)
	Field: Cum+Cpx+Opx+Qtz					
97B-20	Cum+Cpx+Opx+Qtz	730	31	80	80	Cum+Cpx+Opx+Qtz
48B-20	Cum+Cpx+Opx+Qtz	746	30	60	60	Cum+Cpx+Opx+Qtz
79B-40	?Cum+Cpx+Opx+Qtz	760	30	?	5	Cum+Cpx+Opx+Qtz
70A-50	mix	747	13		5	Cum+Cpx+Opx+Qtz
76C-90	Act+Cum+Cpx+Opx+Qtz	730‡	49	5	10	Cum+Cpx+Opx+Qtz +2%(Act)
106A-100	mix	729	13		5	Cum+Cpx+Opx+Qtz
	Field: Cpx+Opx+Qtz					
166A-5	mix	795	10		0	Cpx+Opx+Qtz
165A-10	mix	792‡	10		0	Cpx+Opx+Qtz
107A-20	mix	778	14		0	Cpx+Opx+Qtz
66A-50	Act+Cum+Cpx+Qtz	802	21	85	0	Cpx+Opx+Qtz
72A-90	mix	747	13		0	Cpx+Opx+Qtz
138A-100	Act+?Cum+Cpx+Qtz	769	24	70	0	Cpx+Opx+Qtz
	Anthophyllite data					
183A-0	Anth+Opx+Qtz	715	25	90	99	Anth(+Opx+Qtz)
174A-0	Anth	742	13	99	90	Anth+Opx+Qtz
175B-0	Opx+Qtz	750‡	42	0	5	Anth+Opx+Qtz
170A-0	Anth+Opx+Qtz	782	16	60	0	Opx+Qtz
118C-1.25	Anth+Cum+Ol+Qtz	667‡	60	50	99	Anth+Cum+(Qtz)
102C-2.5	?Anth+Cum+Ol+Qtz	669‡	44	50	99	Anth+Cum+(Ol+Qtz)
109B-2.5	Anth+Cum+Ol+Qtz	715	30	75	99	Anth+Cum+(Qtz)
95B-5	?Anth+Cum+Opx+Qtz	698	30	95	99	Anth+Cum+(Qtz)

*The number following the dash is the Ca content of the charge expressed as mole percent actinolite.
**Phase(s) in parentheses interpreted as metastable.
?Phase may be present.
Amphibole which showed significantly more growth.
‡Temperature variation ± 3°C to ± 5°C; otherwise less than ± 3°C.

+Qtz(+H_2O) is invariant, and is projected as a triangle. This triangle can only touch the field Act at one point; hence the composition of the actinolite is fixed, and, as discussed in a following section, this composition has been determined to be about Act_{85}. Therefore, some third field must separate the fields Act and Act+Cum+Cpx+Qtz along the join $Ca_2Mg_5Si_8O_{23}$–$Ca_2Fe_5Si_8O_{23}$ in Figure 5, and the field Act+Cpx+Qtz appears to be the most reasonable choice. At P_{fluid} = 2000 bars and f_{O_2} defined by the FMQ buffer, actinolite of the composition $Ca_2Fe_{2.5}Mg_{2.5}Si_8O_{22}(OH)_2$ begins to decompose by reaction to clinopyroxene, quartz, and a less calcic actinolite (*i.e.*, enriched in the cummingtonite component). The least calcic composition that amphibole can maintain under these conditions is about 85 mole percent actinolite, which is reached at ~600°C. Above this temperature the actinolitic amphibole begins reacting to Cum+Cpx+Qtz, the ultimate breakdown assemblage of the actinolite. The decom-

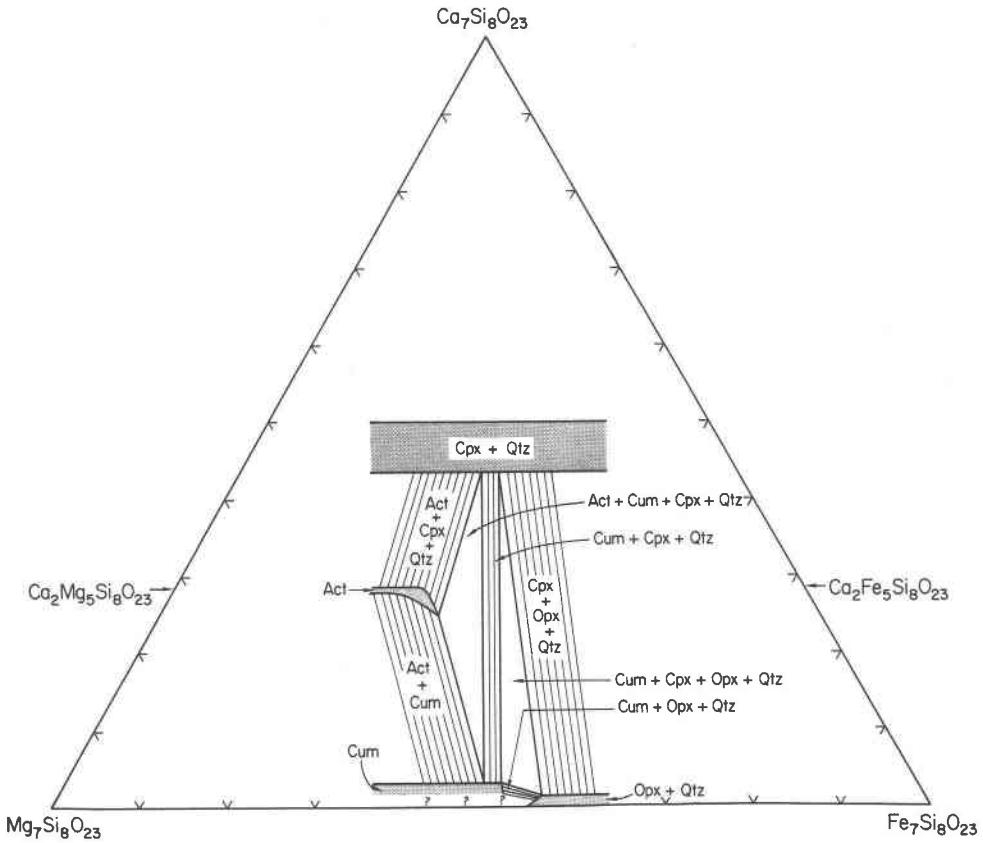

FIG. 5. Schematic isothermal, isobaric diagram showing phase relations encountered in this experimental study. All assemblages exist with a vapor phase. Abbreviations are given in Table 4.

position products of actinolite differ from those found experimentally by Boyd (1959, p. 383) for tremolite (Cpx+Opx+Qtz+H_2O), and by Ernst (1966, p. 57) for ferrotremolite (Cpx+Fa+Mag+Qtz+H_2O) using the FMQ buffer.

The upper boundary of the field Act+Cum+Cpx+Qtz is drawn where the presence of actinolite can no longer be definitely established on X-ray scans. Attempts to produce this assemblage from the assemblages Act+Cum, Act+Cpx+Qtz, and Cpx+Opx+Qtz were unsuccessful. On the bulk composition Act_{100}, cummingtonite—but not actinolite—nucleated and grew from Cpx+Opx+Qtz at 671°C.

The lower boundary of the field Cum+Cpx+Opx+Qtz is placed just above those runs in which orthopyroxene disappeared. All runs in this field are synthesis data; however, most have been rerun and showed either some growth of cummingtonite or no change in phase proportions.

The lower boundary of the field Cpx+Opx+Qtz is placed immediately below runs which produced no amphiboles on synthesis from mixes.

The lower thermal stabilities of the amphiboles were not studied in detail, but amphiboles were observed to grow at the expense of low temperature assemblages. A glass starting material of composition Act_{100} produced Act+Cpx+Qtz at 500°C (51B-100). In contrast, mixes from Act_{100} to Act_{10} initially produced Tc+Cc+Mag+Crist+Ol+traces of amphibole(s). When the charges were rerun, the amphiboles grew and some long runs (≥80 days) produced high yields of amphiboles (*e.g.*, 16E-50, 92D-90, Table 5).

Cummingtonite, in a charge with the bulk composition of Act_{10}, nucleated and grew from Tc+Ol+Cc+Mag+Crist at about 500°C. After 111 days the amphibole comprised 50 percent of the charge and was still growing. Because equilibrium was not reached, the final stable assemblage is not known.

The Actinolite-Cummingtonite Solvus

X-ray Data. It was argued in a preceding section that the Ca contents and Fe:Mg ratios of the clino-

amphiboles can be estimated from their d_{100} spacings and b cell dimensions, respectively. Cell parameters and estimated compositions are given in Table 6, and the estimated Ca contents of clinoamphiboles in multiphase assemblages are shown in Figure 6.

The Ca content of actinolite in the field Act+Cum decreases regularly from about 96 mole percent actinolite at 500°C to about 85 mole percent at 600°C. A straight line appears to give the best fit to the present data on the actinolite limb of the solvus, but the solvus should be somewhat concave toward the Ca-poor side. In the field, Act+Cum+Cpx+Qtz, the Ca content of the actinolite appears to remain constant at about Act_{85} (Fig. 6).

The Ca-poor limb of the solvus is much steeper than the Ca-rich limb. Within the calculated error on d_{100}, the Ca-poor limb could be vertical at about 10 mole percent actinolite.

The Fe-Mg contents of the amphiboles shown in Table 6 are in the general range expected, because all charges have equal mole proportions of FeO and MgO. The uncertainties are relatively large on these estimates; nevertheless cummingtonite is invariably enriched in Fe relative to coexisting actinolite which is consistent with natural assemblages (Fig. 1).

Electron Microprobe Data. To test the technique for analyzing fine powders described by Eugster *et al* (1972), amphiboles of known compositions were analyzed first. Actinolite grains from 73B-100 and cummingtonite grains from 148C-10 are from charges that had been converted largely to a single phase (Table 5); their compositions, therefore, should be that of their charges. The average compositions of the analyzed grains, shown in Table 7, agree quite well with the known compositions of the charges.

The success of analyzing individual phases from multiphase assemblages depends upon being able to disaggregate and disperse the sample. The problem of sample aggregation plagued attempts to analyze individual amphiboles from two-amphibole assemblages. The synthetic amphiboles have an almost acicular habit, and they form mats which usually are impossible to disaggregate. Samples which clearly contained two amphiboles (*e.g.*, 17D-50) yielded only analyses that were near the composition of the charge. Only in sample 13B-50 was it possible to obtain analyses of two distinct populations of amphiboles (Table 7). The Ca contents, especially that of the actinolite, are in good agreement with those expected from the X-ray powder study (Fig. 6); thus the electron microprobe analyses support the credibility of the compositions determined from X-ray data.

TABLE 6. Unit Cell Parameters and Estimated Compositions

Run no.	Temp. (°C)	Assemblage	a(Å)	b(Å)	c(Å)	β(°)	V(Å^3)	d_{100}(Å)	mole* percent actinolite	$\frac{100xFeO}{FeO+MgO}$
					Cummingtonite					
95B-5	698	Anth+Cum	9.528(3)	18.180(10)	5.316(2)	102.08(4)	900.4(5)	9.316	7	48(2)
87B-25	652	Act+Cum	9.545(6)	18.201(12)	5.314(5)	102.28(8)	902.1(8)	9.326	10	52(2)
40C-40	699	Act+Cum+Cpx+Qtz	9.553(7)	18.211(15)	5.315(5)	102.44(8)	903.0(9)	9.329	12	54(3)
16E-50	505	Act+Cum	9.533(7)	18.189(25)	5.317(5)	102.25(9)	901.0(13)	9.316	7.5	50(5)
17D-50	550	Act+Cum	9.536(7)	18.191(13)	5.312(4)	102.26(6)	900.4(8)	9.318	7.5	50(2)
18C-50	582	Act+Cum	9.544(5)	18.165(22)	5.313(3)	102.30(4)	899.9(11)	9.325	10	45(4)
15B-50	603	Act+Cum	9.551(8)	18.195(29)	5.317(4)	102.35(7)	902.7(13)	9.330	12	51(6)
43C-50	665	Act+Cum	9.555(7)	18.198(21)	5.315(3)	102.45(7)	902.5(10)	9.320	8.5	51(4)
55D-10	620	Cum	9.544(5)	18.171(8)	5.316(3)	102.33(5)	900.8(6)	9.324		47(2)
					Actinolite					
16E-50	505	Act+Cum	9.869(5)	18.184(16)	5.301(4)	104.39(7)	921.4(10)	9.560	96	46(6)
17D-50	550	Act+Cum	9.853(7)	18.185(13)	5.294(5)	104.44(8)	918.6(10)	9.542	89.5	46(4)
18C-50	582	Act+Cum	9.854(7)	18.166(18)	5.294(2)	104.44(4)	917.8(9)	9.543	89.5	39(6)
15B-50	603	Act+Cum	9.836(9)	18.193(20)	5.295(4)	104.45(7)	917.5(11)	9.525	83	49(7)
43C-50	665	Act+Cum	9.836(6)	18.189(23)	5.294(4)	104.25(8)	918.0(10)	9.533	86	48(8)
38C-80	556	Act+Cum	9.861(5)	18.206(9)	5.298(2)	104.52(3)	920.8(5)	9.546	90	53(3)
53D-80	651	Act+Cum+Cpx+Qtz	9.835(5)	18.195(9)	5.295(2)	104.38(4)	917.8(5)	9.517	84	50(3)
92D-90	505	Act+Cum	9.883(4)	18.209(10)	5.230(3)	104.56(5)	923.0(6)	9.566	97.5	54(3)
52E-90	650	Act+Cum+Cpx+Qtz	9.846(5)	18.192(9)	5.289(3)	104.33(5)	917.8(5)	9.539	88.5	49(3)
61B-100	650	Act+Cum+Cpx+Qtz	9.836(7)	18.175(16)	5.295(10)	104.38(11)	917.0(14)	9.528	84	43(6)
73B-100	558	Act	9.892(5)	18.191(12)	5.295(3)	104.65(5)	921.9(7)	9.572		48(4)

*Uncertainty ± 4 mole percent

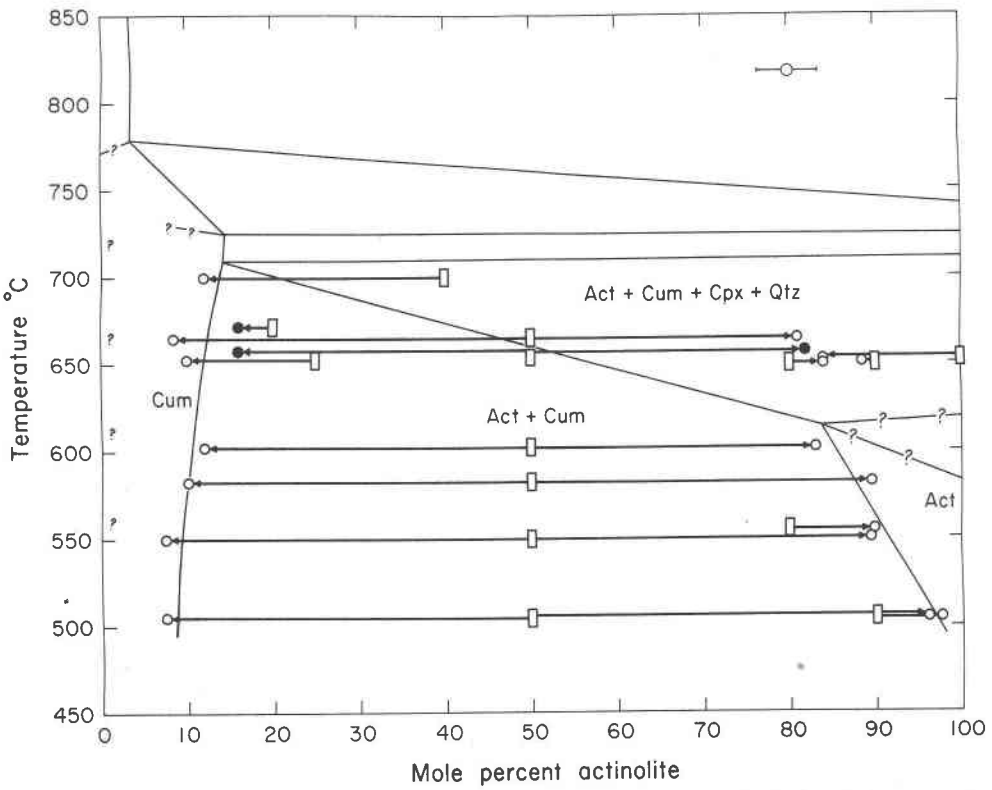

FIG. 6. Compositions of clinoamphiboles in multiphase assemblages. Rectangles indicate bulk composition and temperature of run. Arrows are drawn from the rectangles to circles that indicate the Ca content, expressed as mole percent actinolite, $Ca_2(Mg,Fe)_5Si_8O_{22}(OH)_2$, of the amphiboles. Open circles were determined from X-ray data and the uncertainty, ± 4 mole percent actinolite, is indicated by the bar at top right. Solid circles are electron microprobe data. Uncertainties are ± 4 mole percent for the two amphiboles at 655°C, and ± 8 mole percent for the amphibole at 672°C.

Cummingtonite analyses from 128B-20 are similar to those from 13B-50 (Table 7). However, no analyses of actinolite were obtained from 128B-20, and the phases may not have been completely separated.

Anthophyllite Stability and Anthophyllite-Cummingtonite Relations

Anthophyllite is the only amphibole which has been synthesized on the bulk composition Act_0. There is no optical or X-ray evidence that a monoclinic amphibole is present in any Ca-free runs.

Greenwood (1963) determined that pure-Mg anthophyllite decomposes to enstatite, quartz, and H_2O at ~765°C at P_{H_2O} =2 kbar. In this study the maximum thermal stability of anthophyllite, $Mg_{3.5}Fe_{3.5}Si_8O_{22}(OH)_2$, has been bracketed between 715°C and 742°C (Table 5). As temperature increases, the amphibole reacts to form a more Mg-rich anthophyllite, orthopyroxene, quartz, and H_2O. The boundary between the assemblages Anth+Opx+Qtz and Opx+Qtz has been bracketed between 750°C and 782°C (Table 5). Even the minimum temperature of this bracket seems surprisingly high when compared to Greenwood's data.

Cummingtonite together with anthophyllite crystallizes from unseeded mixes at $Act_{1.25}$ (about 0.2 wt percent CaO). Charges at $Act_{1.25}$, $Act_{2.5}$ and Act_5

TABLE 7. Electron Microprobe Analyses of Synthetic Amphiboles

Run no.*	Assemblage	Phase	Number of Analyses	Mean Ca content**	Mean 100Fe0/(FeO+MgO)
73B-100	Act	Act	10	99(6)***	53(7)
148C-10	Cum	Cum	6	11(2)	54(3)
13B-50	Act+Cum	Act	7	82(4)	50(6)
13B-50	Act+Cum	Cum	4	16(4)	55(3)
128B-20	Act+Cum	Cum	12	16(8)	54(7)

*The number following the dash is the Ca content of the charge expressed as mole percent actinolite.
**Ca content expressed as mole percent actinolite.
***One standard deviation given in parentheses.

were converted to ~99 percent amphibole (Table 5), and the amount of cummingtonite, which appears to increase regularly with increasing Ca content of the charge, seems to be unrelated to either temperature or duration of the run. Both amphiboles grew at the expense of Ol+Qtz and Opx+Qtz, but there was no indication that either grew at the expense of the other. For these reasons it was concluded previously (Cameron, 1971) that a miscibility gap separated anthophyllite and cummingtonite, and at the Fe : Mg ratio of this study, Ca was needed to stabilize cummingtonite.

In more recent experiments[4] cummingtonite has been synthesized in charges with extremely low Ca-contents. The Ca-free mix, Act_0, was seeded with about 10 percent cummingtonite of the composition Act_{10}. Cummingtonite, anthophyllite, orthopyroxene, and quartz grew at the expense of the mix, and the products of this run were used as seeds, again with the mix Act_0, in the next run. In this manner approximately 10-20 percent cummingtonite has been produced in charges containing as little as 40 ppm CaO (bulk composition). However, neither cummingtonite or anthophyllite have been observed to grow at the expense of the other, and their phase relations remain enigmatic.

Discussion of Natural Assemblages

The compositions of natural actinolites (with Fe : Mg near 1) that coexist with cummingtonites can be used to estimate or to put lower limits on metamorphic temperatures, if it is assumed that the actinolite limb of the solvus (Fig. 6) is not significantly affected by the following: (1) changes in P_{total}, (2) Fe : Mg ratios slightly different from those of this study, and (3) small amounts of Na, Mn, Al, Fe^{3+}, *etc*, which are present in most natural actinolites. The estimated uncertainty of ±4 mole percent actinolite in the compositions used to determine the solvus results in a minimum uncertainty of ±35°C in the temperature of equilibration. The temperature uncertainty increases as the natural amphiboles depart from the compositions of this study and as the physical conditions of metamorphism depart from the experimental conditions.

[4] These experiments were made at the State University of New York at Stony Brook.

TABLE 8. Mineral Assemblages of the Wabush Iron Formation, Labrador and Quebec

Assemblage*	Wabush Lake Klein (1966)	Bloom Lake Mueller (1960)	Mount Reed Butler (1969)
Act	X	X	X**
Cum	X	X	X
Act+Cum	X	X	
Act+Cum+Cpx+Qtz		X	
Cum+Cpx+Qtz	X		X
Cum+Opx+Qtz	X		X
Cum+Cpx+Opx+Qtz			X
Cpx+Opx+Qtz			X

*All ± quartz ± carbonate(s) ± magnetite ± graphite ± sulfides
**Actinolites very Mg-rich (Fe/Mg+Fe≤0.20) and most coexist with hematite
X Common assemblages

Wabush Iron Formation, Canada

The petrology of the metamorphosed Precambrian Wabush Iron Formation in Labrador and Quebec has been investigated in unusual detail by Mueller (1960), Kranck (1961), Klein (1966), and Butler (1969). The mineral assemblages from the Wabush Iron Formation that are relevant to this study are summarized in Table 8.

Klein found coexisting Act+Cum(+Cpx+Mag+Carb) at one locality near Wabush Lake (analyses in Klein, 1968, no. 4-6). The calcic amphibole has a composition of 91 mole percent actinolite, which suggests a temperature of equilibration of ~ 550°C. Based on the melting curve of granite, Klein (1966, p. 294) estimated the maximum temperature of metamorphism to be "below about 600°C." The metamorphism is of the kyanite-staurolite zone, and the presence of kyanite at 550°-600°C suggest $P_{total} \geq 5$ kbar (Richardson, Gilbert, and Bell, 1969).

About 20 miles to the southwest at Bloom Lake (Mueller, 1960), the calcic amphiboles coexisting with cummingtonite range in composition from 82-92 mole percent actinolite, thus suggesting metamorphic temperatures between ~ 550°C and 600°C. Neither Kranck (1961) nor Butler (1969) found coexisting actinolite-cummingtonite in the Mount Reed area, approximately 70 miles southwest of Bloom Lake. Because of the abundance of pyroxenes at Mount Reed, Butler concludes that the grade of metamorphism increases from the Wabush and Bloom Lake areas southwest to the Mount Reed area. A comparison of the mineral assemblages in Table 8 and those in Figure 4 indicates that the mineral assemblages reported by Butler are those expected if the metamorphic grade is indeed higher to the southwest.

The assemblage Mg-rich Act+Cpx+Opx+Qtz (+Carb+Mag+Hem) is reported by Butler (1969, p. 75, assemblage 274). This assemblage is consistent

with the decomposition reaction Tre→Cpx+Opx +Qtz+H_2O studied experimentally by Boyd (1959). Kranck (1961) recognized, however, that intermediate Fe-Mg actinolite decomposes to Cum+Cpx+Qtz+H_2O. He did not find the assemblage Act+Cum+Cpx+Qtz, but the assemblage Cum+Cpx+Qtz is common. The stable tieline between cummingtonite and clinopyroxene plus quartz precludes a tieline between actinolite and orthopyroxene plus quartz (Fig. 5). The conclusion that the decomposition assemblage of the intermediate Fe-Mg actinolites is Cum+Cpx+Qtz was reached independently in this study.

Iron Formation, Ruby Mountains, Montana

Coexisting actinolites and cummingtonites from the metamorphosed iron formation of the Ruby Mountains are of particular interest because of the conspicuous abundance of exsolution lamellae in some of the amphiboles (Ross *et al,* 1969). The rocks are composed principally of amphiboles, magnetite, and quartz with minor amounts of apatite, chlorite, and biotite. Ross *et al* report that cummingtonite host crystals contain few exsolution lamellae of actinolite, whereas cummingtonite lamellae are numerous in actinolite host crystals. From these observations they concluded that the actinolite-cummingtonite solvus is asymmetric with a very steep cummingtonite limb. This shape has been confirmed in this experimental study.

The actinolite in some of the Ruby Mountain samples appears to have contained considerably more cummingtonite in solid solution than would be expected from this study. In some samples the solubility of cummingtonite in actinolite is as much as 50 percent, which compares with a maximum of about 15 percent shown in Figure 6. The greater solid solution is not an effect of chemical components not present in the synthetic system; Papike, Cameron, and Shaw (1973) found that in the Ruby Mountain samples the solubility of cummingtonite in actinolite decreases with increasing Na and Al content. Although the solvus in Figure 6 has not been reversed experimentally, it is unlikely that the synthetic actinolite coexisting with cummingtonite is *less* calcic than the stable compositions. The greater solid solution suggests that the Ruby Mountain samples were metamorphosed at higher temperatures and higher P_{H_2O} than the experimental conditions of this study. Increased P_{H_2O} should raise the upper boundary of the field Act+Cum (Fig. 4), thereby exposing more of the solvus and allowing increased solubility of cummingtonite in actinolite.

Decomposition of Ferrotremolite and Mineral Assemblages from an Iron Formation, Gulf of Bothnia, Finland

Ernst (1966) concluded from his experimental studies that pure-Fe ferrotremolite decomposes to Cpx+Fa+Mag+Qtz+H_2O on the FMQ buffer. At the same conditions another possible breakdown assemblage is Grun+Cpx+Qtz+H_2O, which is analogous to the decomposition products of actinolite found in this study. Ernst did not report the presence of grunerite in any of his runs, but the synthesis of grunerite is known to be difficult.

Natural assemblages should provide information on the decomposition products of ferrotremolite. Hytönen (1968) described samples which contain mineral assemblages relevant to this problem in drill cores taken from beneath the Gulf of Bothnia, Finland, and the author obtained some of these samples.

Seven of the nine samples examined contain the assemblage Ferrotre+Grun+Hd±Fa±Mag±sulfides; the assemblages lack quartz. The remaining two samples contain Ferrotre+Grun+Hd+Qtz+sulfides. All phases were observed in mutual contact, and both the ferrotremolite and grunerite contain fine ($\bar{1}01$) exsolution lamellae. Analyses of the ferromagnesian minerals are shown in Table 9.

To the knowledge of the author, the ferrotremolite in Table 9 is the most Fe-rich one which has been reported co-existing with a possible decomposition assemblage, and apparently the assemblage Ferrotre+Hd+Fa(and/or Mag)+Qtz has never been reported. These observations suggest, but do not prove, that the *stable* reaction for the decomposition of the pure-Fe amphibole is Ferrotre→Grun+Hd+Qtz+H_2O at f_{O_2} defined by the FMQ buffer.

TABLE 9. Electron Microprobe Analyses of Coexisting Minerals from a Metamorphosed Iron Formation, Gulf of Bothnia, Finland

	Ca-pyroxene	Ferrotremolite		Grunerite
		Core	Rim	
SiO_2	50.94	47.48	50.04	50.08
Al_2O_3	0.33	4.04	2.46	0.28
FeO*	25.11	31.22	30.63	43.22
MgO	3.34	3.61	4.36	3.88
CaO	21.28	10.47	10.61	0.90
Na_2O	0.38	0.89	0.57	0.05
K_2O	0.00	0.33	0.18	0.02
Total	101.38	98.02	98.84	98.43

*Total Fe as FeO
Sample from drill core No. 1, depth 91.5 m.

Acknowledgments

This paper is based on a Ph.D. dissertation submitted to the Faculty of the Virginia Polytechnic Institute and State University. The writer gratefully acknowledges the guidance and advice of M. C. Gilbert who suggested this study. Discussions with D. M. Burt and H. S. Yoder were also particularly helpful. An earlier version of this manuscript was substantially improved by the constructive criticisms of F. D. Bloss, P. H. Ribbe, M. Cameron, and W. G. Ernst.

This research was supported by NSF Grant GA-12479 to M. C. Gilbert, and a Predoctoral Fellowship at the Geophysical Laboratory, Carnegie Institution of Washington. The writer also expresses his thanks to A. E. Bence for advice regarding the electron microprobe analyses, and to D. H. Lindsley for access to the hydrothermal laboratory at SUNY, Stony Brook.

Samples from the Gulf of Bothnia were obtained through the courtesy of Dr. Kai Hytönen, Geological Survey of Finland, and Dr. Juhani Nuutilainen of the Rautaruukki Company.

References

Appleman, D. E., F. R. Boyd, G. M. Brown, W. G. Ernst, G. V. Gibbs, and J. V. Smith (1966) *Short Course on Chain Silicates.* Am. Geol. Inst., Washington, D.C.

Bence, A. E., and A. L. Albee (1968) Empirical correction factors for the electron microanalysis of silicates and oxides. *J. Geol.* **76,** 382–403.

Borg, I. Y., and D. K. Smith (1969) Calculated X-ray powder patterns for silicate minerals. *Geol. Soc. Am. Mem.* **122,** 896 p.

Boyd, F. R. (1959) Hydrothermal investigation of amphiboles. In, P. H. Abelson, Ed., *Researches in Geochemistry.* John Wiley and Sons, New York.

Butler, P. (1969) Mineral compositions and equilibria in the metamorphosed iron formation of the Gagon Region, Quebec, Canada. *J. Petrol.* **10,** 56–101.

Cameron, K. L. (1971) Amphibole phase relations along the join $Mg_{3.5}Fe_{3.5}Si_8O_{22}(OH)_2$–$Ca_2Mg_{2.5}Fe_{2.5}Si_8O_{22}(OH)_2$. *Carnegie Inst. Wash. Year Book,* **70,** 145–150.

Colville, P., W. G. Ernst, and M. C. Gilbert (1966) Relationships between cell parameters and chemical compositions of monoclinic amphiboles. *Am. Mineral.* **51,** 1727–1754.

Ernst, W. G. (1966) Synthesis and stability relations of ferrotremolite. *Am. J. Sci.* **264,** 37–65.

——— (1968) *Amphiboles.* Springer-Verlag New York Inc., New York, 125 p.

Eskola, P. (1950) Paragenesis of cummingtonite and hornblende from Muuruvesi, Finland. *Am. Mineral.* **35,** 729–734.

Eugster, H. P., and D. R. Wones (1962) Stability relations of the ferruginous biotite, annite. *J. Petrol.* **3,** 82–125.

———, A. L. Albee, A. E. Bence, J. B. Thompson, and D. R. Waldbaum (1972) The two-phase region and excess mixing properties of paragorite-muscovite crystalline solutions. *J. Petrol.* **13,** 147–179.

Evans, H. T., D. E. Appleman, and D. S. Handwerker (1963) The least squares refinement of crystal unit cell with powder diffraction data by an automatic computer indexing method (abstr.). *Progr. Annu. Meet. Am. Crystallogr. Assoc.,* 42–43.

Greenwood, H. J. (1963) The synthesis and stability of anthophyllite. *J. Petrol.,* **4,** 317–351.

Hadidiacos, C. G. (1969) Solid-state temperature controller. *J. Geol.* **77,** 365–367.

Hellner, E., and K. Schürmann (1966) Stability of metamorphic amphiboles, The tremolite-ferroactinolite series. *J. Geol.* **74,** 322–331.

Hinrichsen, Th. (1967) Uber den stabilitatsbereich der Mg-Fe^{2+}-Al-mischkristallreihe rhombischer hornblenden. *Neues Jahrb. Mineral. Monatsh.,* 257–270.

Hytönen, K. (1968) A preliminary report on an iron-rich formation near Raahe in the Gulf of Bothnia, Finland. *Bull. Geol. Soc. Finland,* **40,** 135–144.

Johannsen, A. (1937) *A Descriptive Petrography of Igneous Rocks,* Vol. 3. University of Chicago Press, Chicago.

Klein, Cornelis (1966) Mineralogy and petrology of the metamorphosed Wabush iron formation, southwestern Labrador. *J. Petrol.* **7,** 246–305.

——— (1968) Coexisting amphiboles. *J. Petrol.* **9,** 281–330.

Klein, C., and D. R. Waldbaum (1967) X-ray crystallographic properties of the cummingtonite-grunerite series. *J. Geol.* **75,** 379–392.

Kranck, S. H. (1961) A study of phase equilibrium in a metamorphic iron formation. *J. Petrol.* **2,** 137–184.

Layton, W., and R. Phillips (1960) The cummingtonite problem. *Mineral. Mag.* **32,** 659–663.

Mueller, R. F. (1960) Compositional characteristics and equilibrium relations in mineral assemblages of a metamorphosed iron formation. *Am. J. Sci.* **258,** 449–497.

Papike, J. J., K. L. Cameron, and K. W. Shaw (1973) Chemistry of coexisting actinolite-cummingtonite and hornblende-cummingtonite from metamorphosed iron formation. *Geol. Soc. Am. Abstr. Progr.* **5,** 763–764.

Popp, R. K., M. C. Gilbert, and J. R. Craig (1974) Cell parameters of synthetic amphiboles on the join Mg_7 ···– $Fe_7Si_8O_{22}(OH)_2$ (abstr.). *Trans. Am. Geophys. Union,* **55,** 464.

Richardson, S. W., M. C. Gilbert, and P. M. Bell (1969) Experimental determination of kyanite-andalusite and andalusite-sillimanite equilibrium; the aluminum silicate triple point. *Am. J. Sci.* **267,** 259–272.

Robinson, P., and H. W. Jaffe (1969) Chemographic exploration of amphibole assemblages from central Massachusetts and southwestern New Hampshire. *Mineral. Soc. Am. Spec. Pap.* **2,** 251–274.

———, M. Ross, and H. W. Jaffe (1971) Composition of the anthophyllite-gedrite series, comparisons of gedrite and hornblende, and the anthophyllite-gedrite solvus. *Am. Mineral.* **56,** 1005–1041.

Ross, M., J. J. Papike, and K. W. Shaw (1969) Exsolution textures in amphiboles as indicators of subsolidus thermal histories. *Mineral. Soc. Am. Spec. Pap.* **2,** 275–299.

Schürmann, K. (1967) Hydrothermale experimentelle untersuchungen an metamorphen monoklinen hornblenden: teil I: Zur stabilitat der cummingtonite. *Neues Jahrb. Mineral. Monatsh.,* 270–284.

——— (1968) Synthesis and stability field of cummingtonite. *Int. Mineral. Assoc. 5th Gen. Meet. Cambridge 1966,* 255–260.

Stout, J. H. (1971) Four coexisting amphiboles from Telemark, Norway. *Am. Mineral.* **56,** 212–224.

Tuttle, O. F. (1949) Two pressure vessels for silicate-water studies. *Geol. Soc. Am. Bull.* **60,** 1727–1729.

Whittaker, E. J. W. (1960) The crystal chemistry of the amphiboles. *Acta Crystallogr.* **13,** 291–298.

Manuscript received, September 16, 1974; accepted for publication, January 13, 1975.